Electronic Supplementary Material (ESI) for Organic Chemistry Frontiers.

1,2-Migration in the Reactions of Ruthenium Vinyl Carbene with Propargyl Alcohols

Xiaoxi Zhou,[a] Chunhong Zhang,[a] Yumei Lin,[a] Xumin He,[a] Yan Zhang,[b] Jianbo Wang,[b, c] and Haiping Xia*[a]

[a] State Key Laboratory for Physical Chemistry of Solid Surfaces, Department of Chemistry, College of Chemistry and Chemical Engineering, Xiamen University, Xiamen, 361005, China. E-mail: hpxia@xmu.edu.cn;
Fax: 86-0592-2186628; Tel: 86-0592-2186658;
[b] Beijing National Laboratory of Molecular Sciences (BNLMS), Key Laboratory of Bioorganic Chemistry and Molecular Engineering of Ministry of Education, College of Chemistry, Peking University, Beijing, 100871, China;
[c] State Key Laboratory of Organometallic Chemistry, Chinese Academy of Sciences, Shanghai, 200032, China.

Contents

1. Crystallographic details

Crystallographic Analysis: All single crystals were mounted on glass fibers and transferred into a cold stream of nitrogen. Diffraction data for **2** were obtained on a Rigaku R-AXIS SPIDER IP CCD area detector at 173(2) K, with graphite-monochromated Mo Kα radiation (λ = 0.71073 Å). Diffraction data for **3**, **5**, **6** were collected on an Oxford Gemini-S Ultra charge coupled device (CCD) diffractometer at 173(2) K, with monochromated Mo Kα radiation (λ = 0.71073 Å). Semi-empirical or multi-scan absorption corrections (SADABS) were applied.[1] Structures were solved by the Patterson function, completed by subsequent difference Fourier map calculations, and refined by full matrix least-squares on F^2 using the SHELXTL program package.[2] Non-hydrogen atoms were refined anisotropically unless otherwise stated. Hydrogen atoms were placed at idealized positions and assumed the riding model. For all the complexes, crystals suitable for X-ray diffraction were grown from CH_2Cl_2 solution layered with hexane.

[1] G. M. Sheldrick, *SADABS, Program for semi-empirical absorption correction*; University of Göttingen: Göttingen, Germany, 1997.

[2] G. M. Sheldrick, *SHELXTL*; Siemens Analytical X-ray Systems: Madison, Wisconsin, USA.

Table 1 Crystal data and structure refinement for **2**, **3**, **5** and **6**.

complex	**2**·3CH_2Cl_2·	**3**·4CH_2Cl_2	**5**·1.5CH_2Cl_2	**6**·CH_2Cl_2
formula	$C_{59}H_{48}BCl_2F_4NOP_2Ru$	$C_{54}H_{46}BCl_2F_4NOP_2Ru$	$C_{48}H_{42}BCl_2F_4NOP_2Ru$	$C_{50}H_{44}BCl_2F_4NO_2P_2Ru$
Mr	1362.48	1385.34	1096.93	1080.51
crystal system	Triclinic	Triclinic	Monoclinic	Monoclinic
space group	P-1	P-1	P2(1)/c	P2(1)/c
a, Å	12.818(3)	13.1474(8)	23.3968(8)	13.0587(4)
b, Å	14.788(7)	13.1912(7)	10.7057(4)	25.8151(7)
c, Å	16.847(7)	20.2329(12)	19.1358(7)	14.6635(4)
a, °	72.67(3)	80.722(5)	90	90
β, °	86.64(3)	87.504(5)	90.758(3)	95.876(3)
γ, °	84.12(3)	63.196(6)	90	90
V, $Å^3$	3031.1(11)	3089.3(3)	4792.7(3)	4917.3(2)
Z	2	2	4	4

dcalcd, g cm^{-3}	1.493	1.489	1.52	1.46
F(000)	1384	1404	2228	2200
crystal size, mm	0.3× 0.25× 0.15	0.4×0.3×0.2	0.4×0.3×0.1	0.3×0.2×0.08
θ range, °	3.04 - 25.00	2.72-25.00	2.78-25.00	2.75-25.00
reflns collected	23927	23097	21647	22197
indep reflns	10655	10874	8438	8656
data/restraints/params	10655 / 0 / 721	10874 / 0 / 703	8438 / 0 / 582	8656 / 0 / 586
GOF on F^2	0.974	1.138	1.355	1.001
$R_1/wR_2(I > 2\sigma(I))$	0.0598/0.1792	0.0619/0.1691	0.0448/0.1173	0.0712/0.1618
R_1/wR_2(all) data)	0.0776/0.2180	0.0788/0.1808	0.0560/0.1221	0.0915/0.1736
largest peak/hole [e $Å^{-3}$]	2.352/-1.238	1.185/-1.296	1.047/-1.053	2.195/-1.960

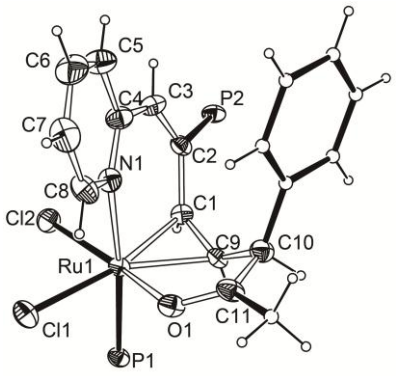

Figure S1-1 Molecular structure for complex **3** (ellipsoids at the 50% probability level). The phenyl rings in PPh_3 groups and the counter anion are omitted for clarity. Selected bond distances [Å] and angles [°]: Ru(1)–O(1) 2.111(3), O(1)–C(11) 1.235(6), C(11)–C(10) 1.509(6), C(9)–C(10) 1.537(6), C(1)–C(9) 1.396(6), C(2)–C(1) 1.482(6), C(2)–C(3) 1.343(6), C(3)–C(4) 1.462(7), N(1)–C(4) 1.348(6), Ru(1)–C(1) 2.150(4), Ru(1)–C(9) 2.158(4), Ru(1)–N(1) 2.182(4), O(1)–Ru(1)–C(9) 74.67(14), O(1)–Ru(1)–C(1) 109.24(15), O(1)–C(11)–C(10) 119.0(4), C(11)–C(10)–C(9) 105.9(4), C(10)–C(9)–Ru(1) 110.5(3), C(9)–C(1)–C(2) 131.2(4), C(3)–C(2)–C(1) 128.9(4), C(2)–C(3)–C(4) 129.4(5), N(1)–C(4)–C(3) 120.9(4), O(1)–Ru(1)–N(1) 83.05(13), C(4)–N(1)–Ru(1) 127.4(3), C(1)–Ru(1)–C(9) 37.81(16).

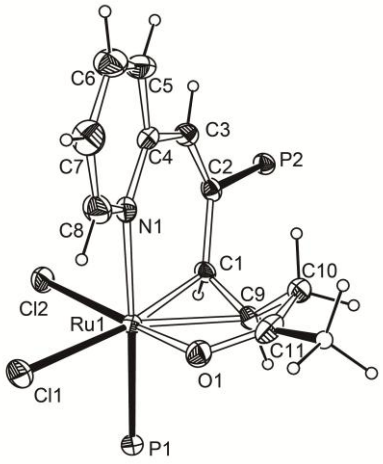

Figure S1-2 Molecular structure for complex **5** (ellipsoids at the 50% probability level). The phenyl rings in PPh_3 groups and the counter anion are omitted for clarity. Selected bond distance [Å] and angles [ ]: Ru(1)–O(1) 2.108(2), O(1)–C(11) 1.231(5), C(11)–C(10) 1.483(5), C(9)–C(10) 1.501(5), C(1)–C(9) 1.398(5), C(2)–C(1) 1.486(5), C(2)–C(3) 1.334(5), C(3)–C(4) 1.465(5), N(1)–C(4) 1.364(4), Ru(1)–C(1) 2.156(3), Ru(1)–C(9) 2.145(3), Ru(1)–N(1) 2.202(3), O(1)–Ru(1)–C(9) 74.63(11), O(1)–Ru(1)–C(1) 109.26(12), O(1)–C(11)–C(10) 118.1(3), C(11)–C(10)–C(9) 107.5(3), C(10)–C(9)–Ru(1) 107.5(2), C(9)–C(1)–C(2) 124.3(3), C(3)–C(2)–C(1) 129.2(3), C(2)–C(3)–C(4) 130.1(3), N(1)–C(4)–C(3) 121.1(3), O(1)–Ru(1)–N(1) 79.72(10), C(4)–N(1)–Ru(1) 128.0(2), C(9)–Ru(1)–C(1) 37.92(12).

2. NMR spectra

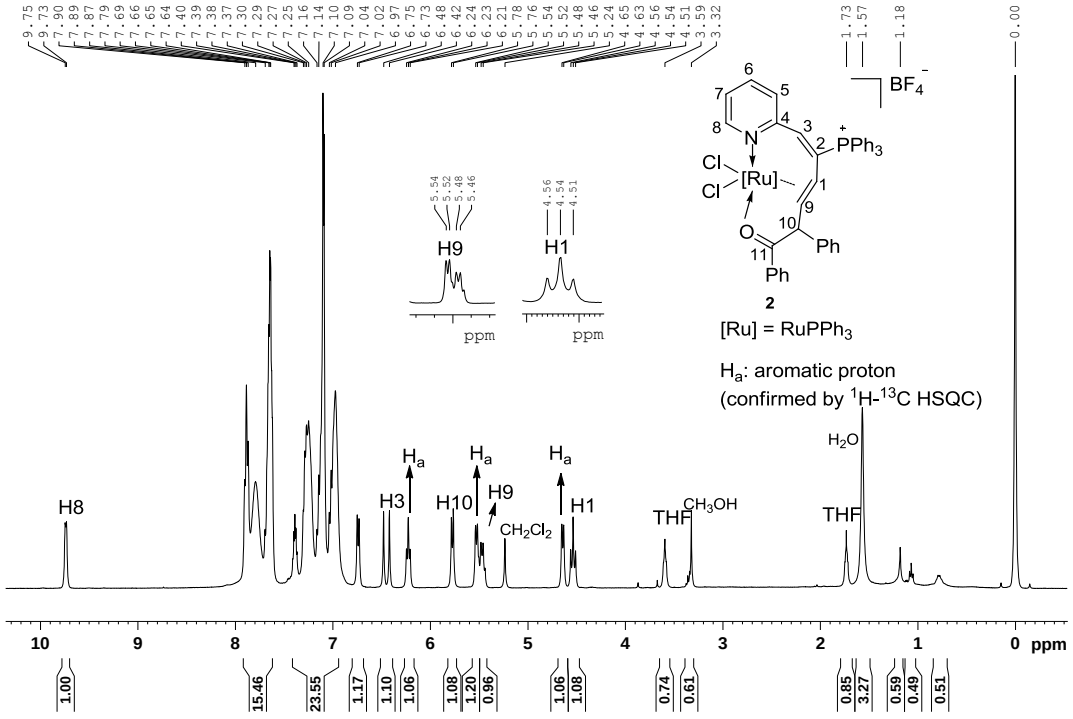

Figure S2-1 The ^1H NMR spectrum of complex **2** in CD_2Cl_2 at 400.13 MHz.

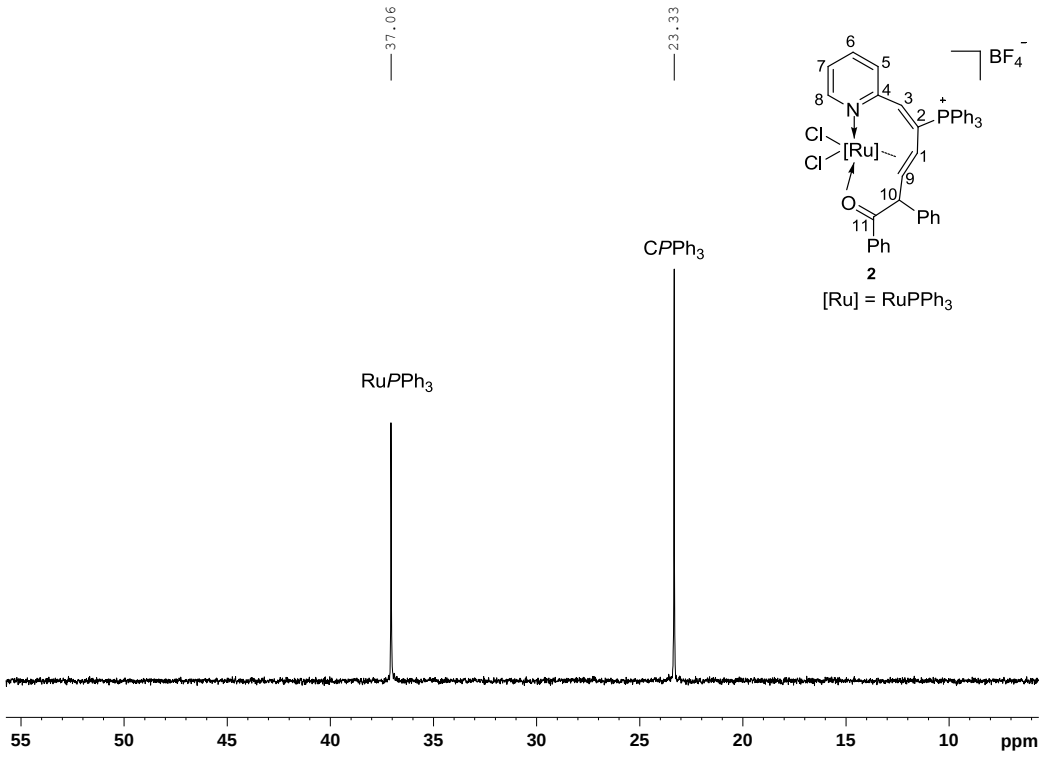

Figure S2-2 The ^{31}P NMR spectrum of complex **2** in CD_2Cl_2 at 161.96 MHz

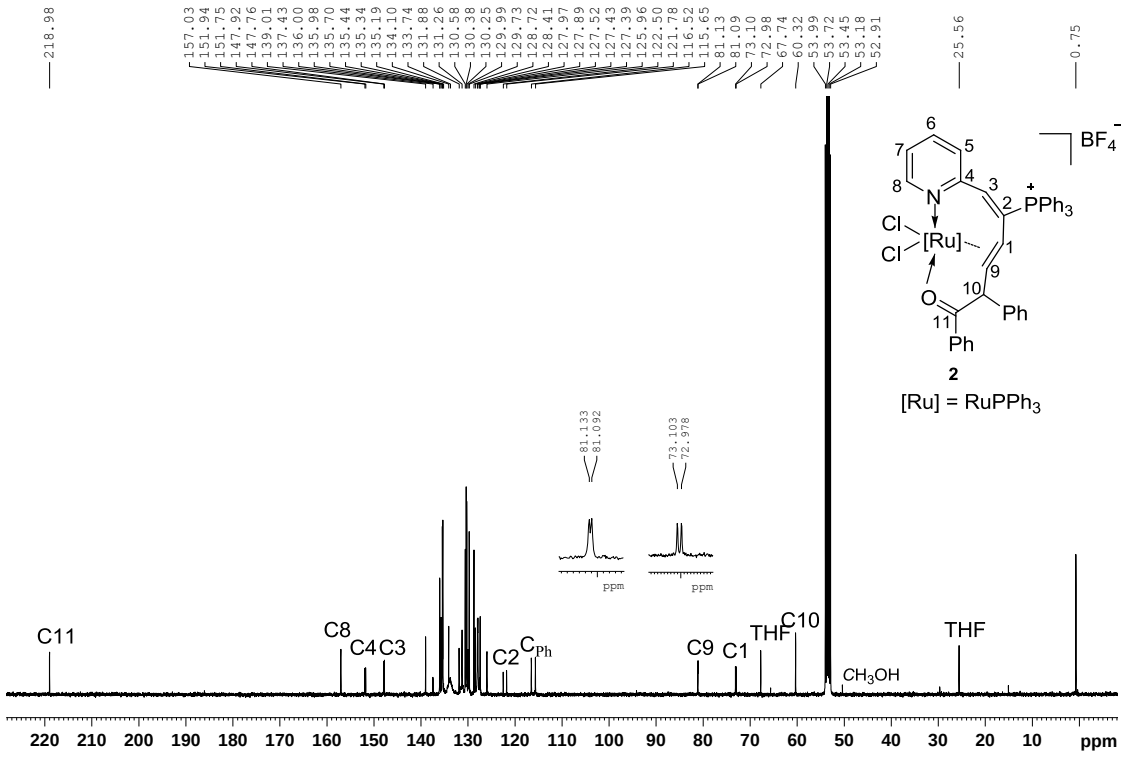

Figure S2-3 The ^{13}C NMR spectrum of complex **2** in CD_2Cl_2 at 100.63 MHz.

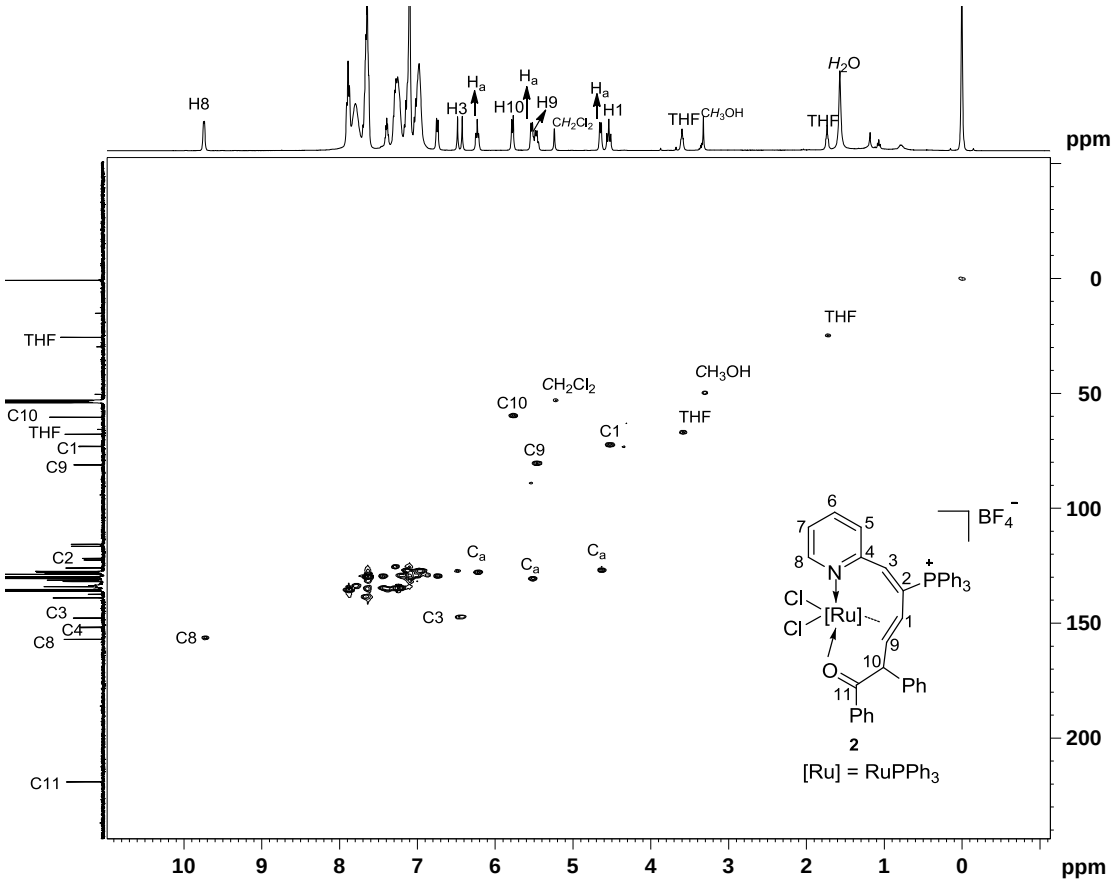

Figure S2-4 The ^{1}H–^{13}C HSQC of complex **2** in CD_2Cl_2 at 100.63 MHz.

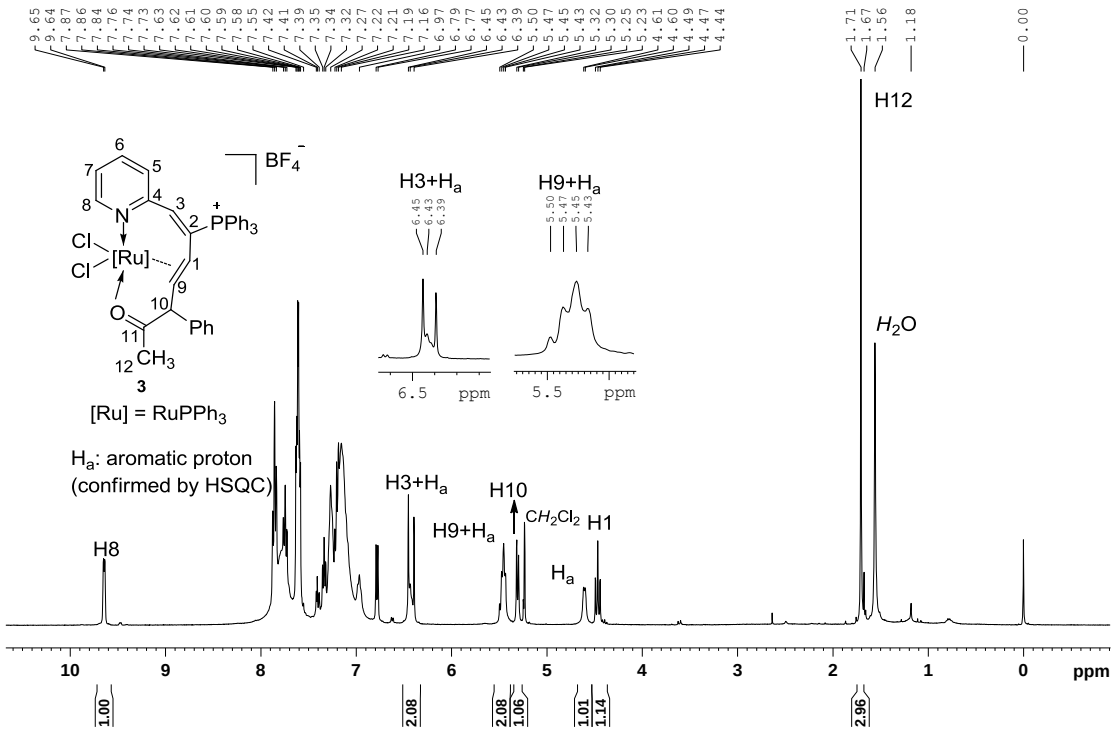

Figure S2-5 The ^{1}H NMR spectrum of complex **3** in CD_2Cl_2 at 400.13 MHz.

Additional peaks: 9.47, 6.62, 5.24, 4.40, 3.61, 1.67 ppm (a minor unidentified byproduct).

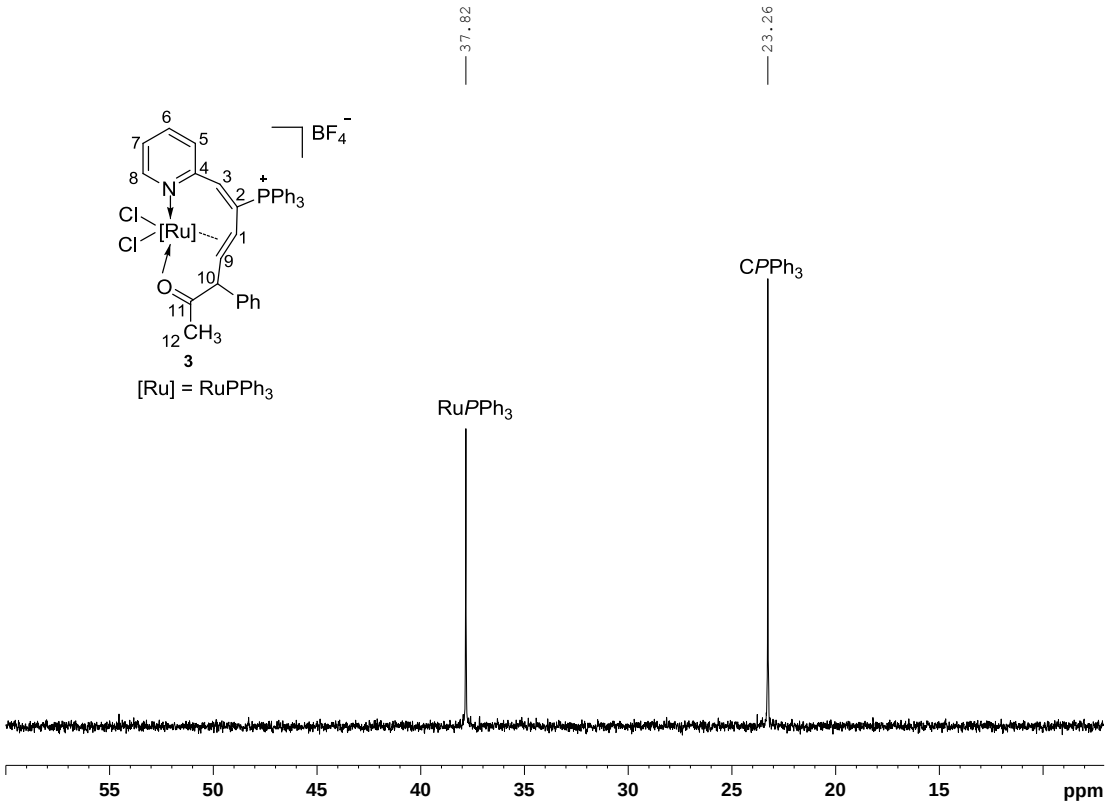

Figure S2-6 The ^{31}P NMR spectrum of complex **3** in CD_2Cl_2 at 161.96 MHz

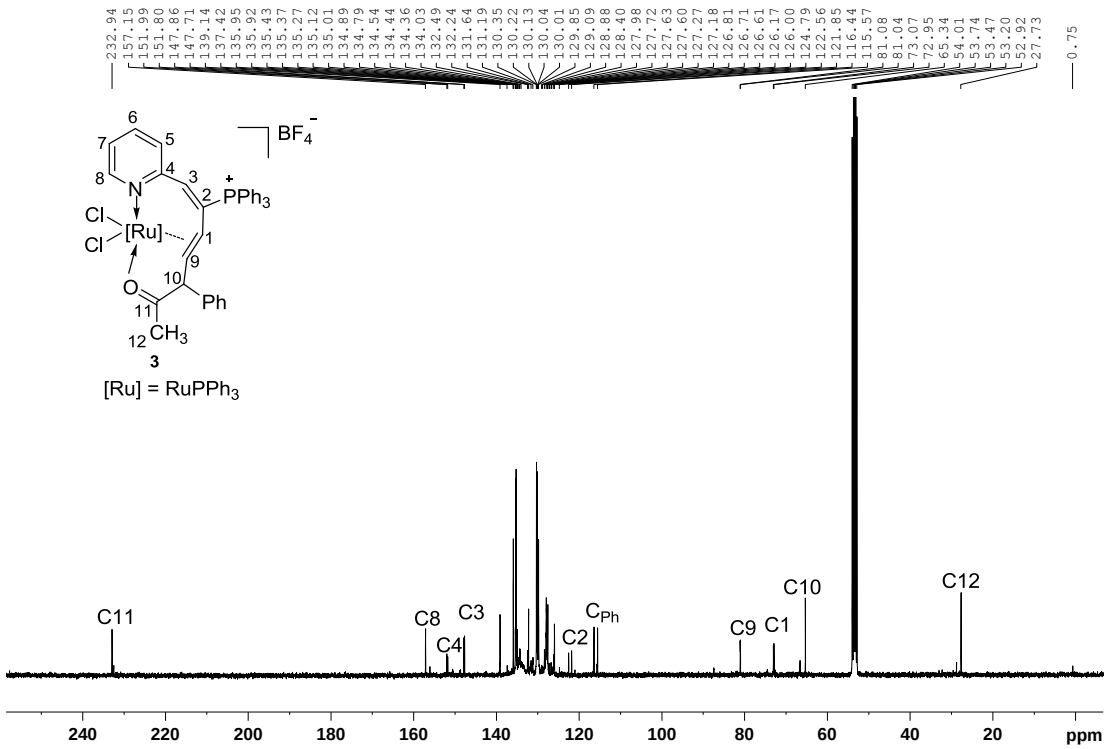

Figure S2-7 The ^{13}C NMR spectrum of complex **3** in CD_2Cl_2 at 100.63 MHz.

Additional peaks: 232.52, 156.10, 150.52, 148.76, 116.12, 87.48, 74.56, 66.67, 28.87 ppm (a minor unidentified byproduct).

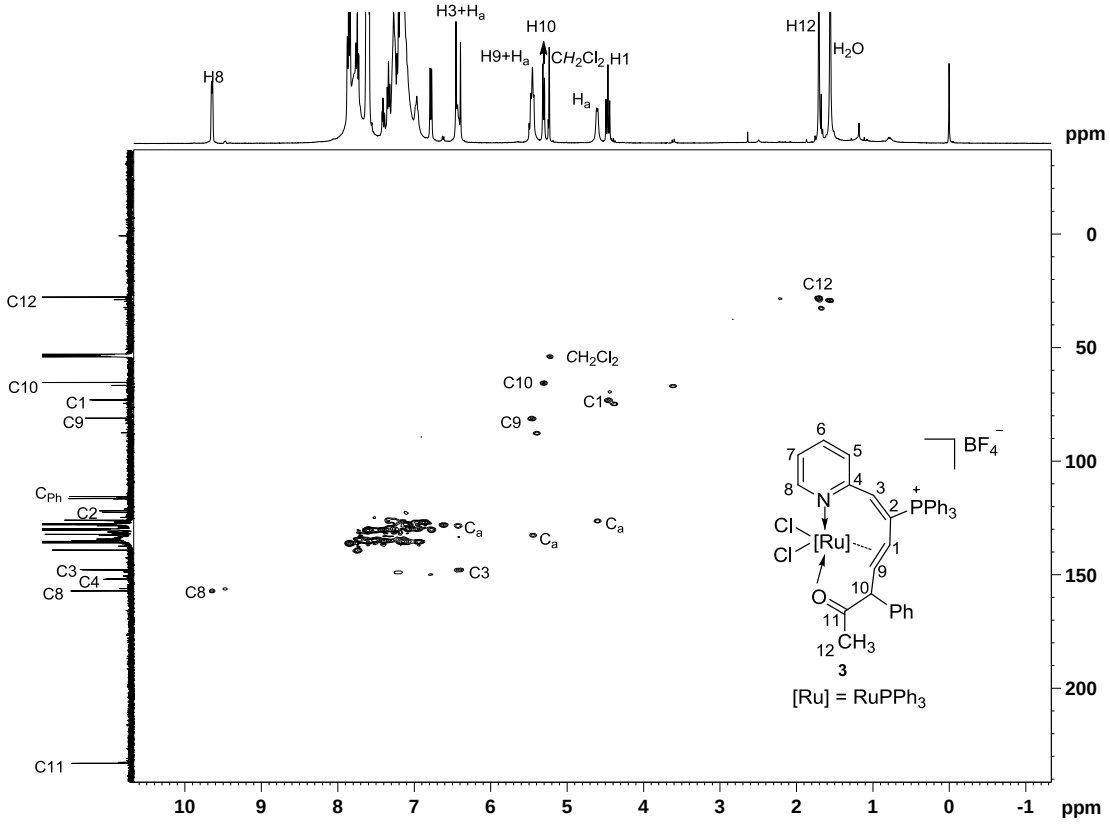

Figure S2-8 The ^{1}H–^{13}C HSQC spectrum of complex **3** in CD_2Cl_2 at 100.63 MHz.

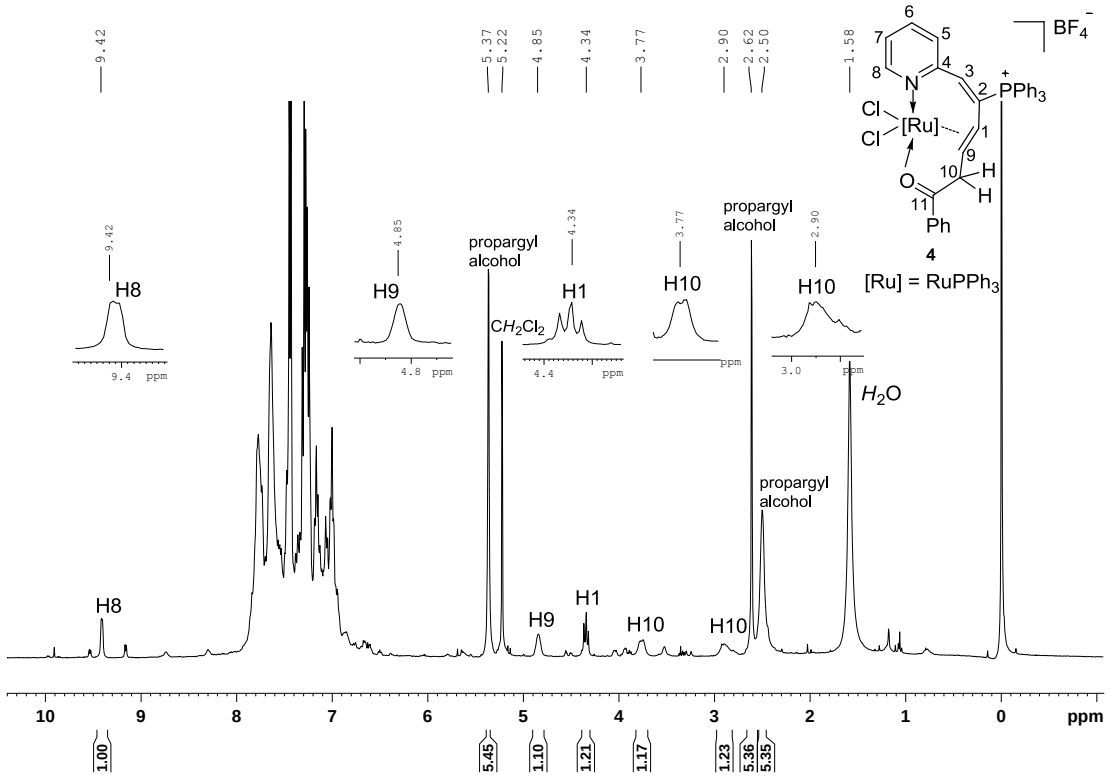

Figure S2-9 The in-situ ^{1}H NMR spectrum of complex **4** in CD_2Cl_2 at 400.13 MHz.

Additional peaks: peaks for other byproducts.

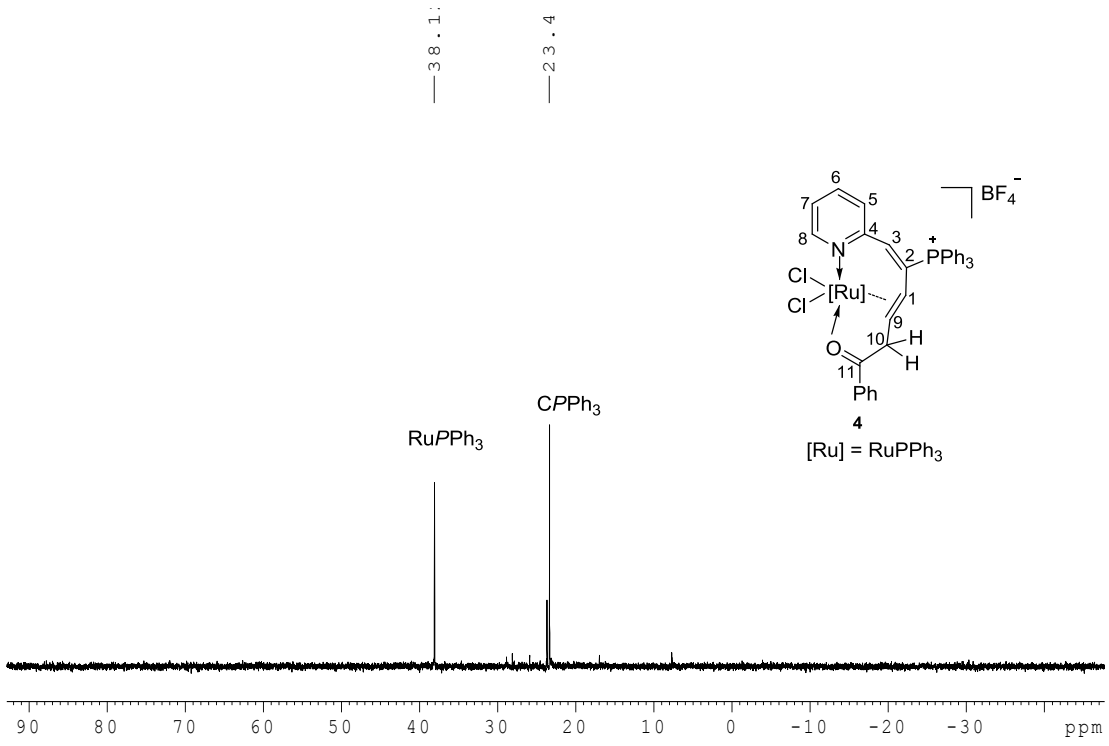

Figure S2-10 The in-situ ^{31}P NMR spectrum of complex **4** in CD_2Cl_2 at 161.96 MHz.

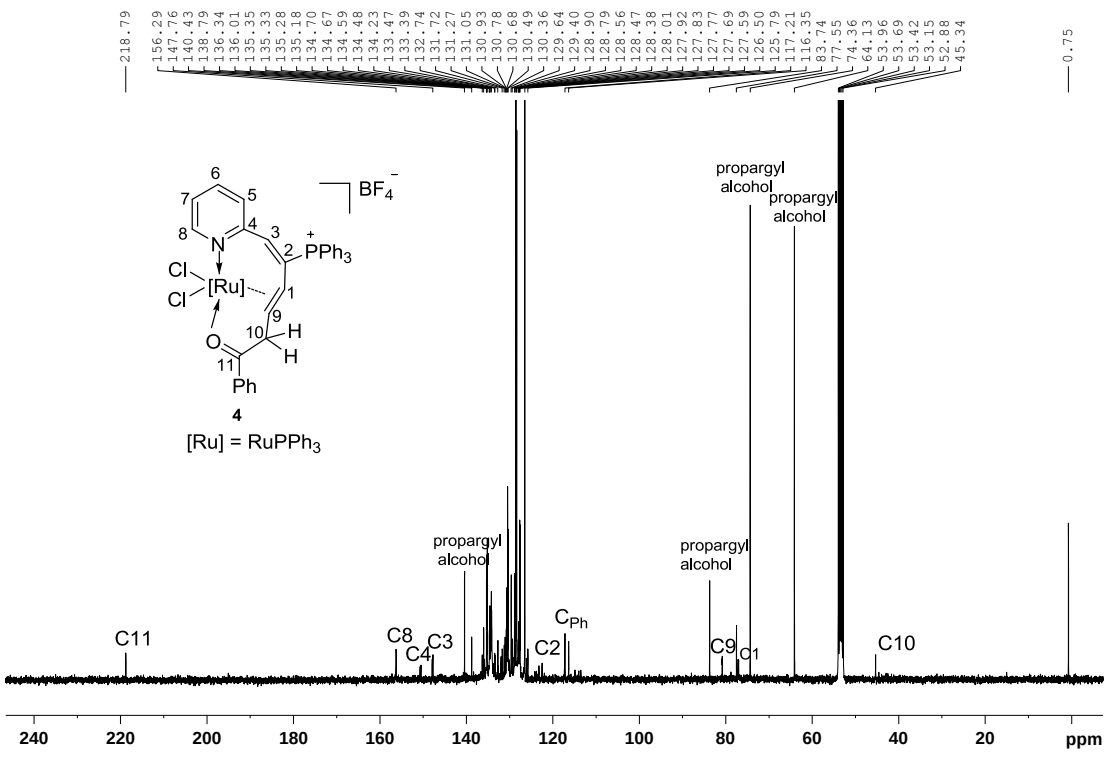

Figure S2-11 The in-situ ^{13}C NMR spectrum of complex **4** in CD_2Cl_2 at 100.63 MHz.

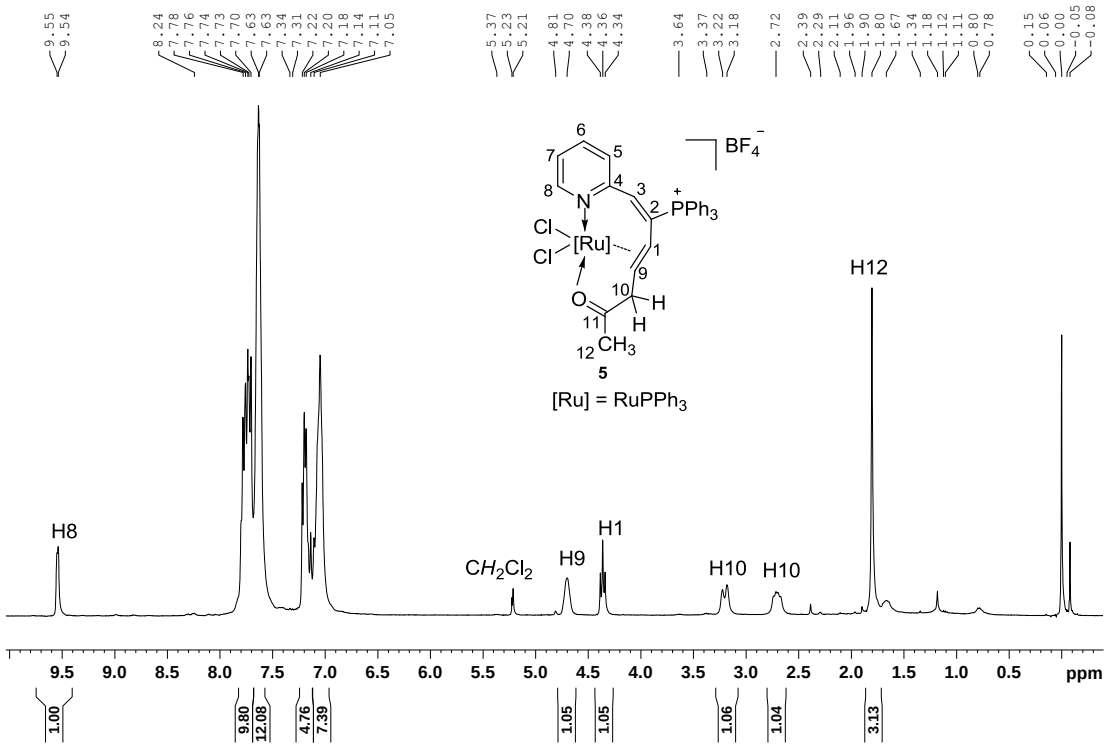

Figure S2-12 The ^{1}H NMR spectrum of complex **5** in CD_2Cl_2:$CDCl_3$ = 3:5 at 400.13 MHz.

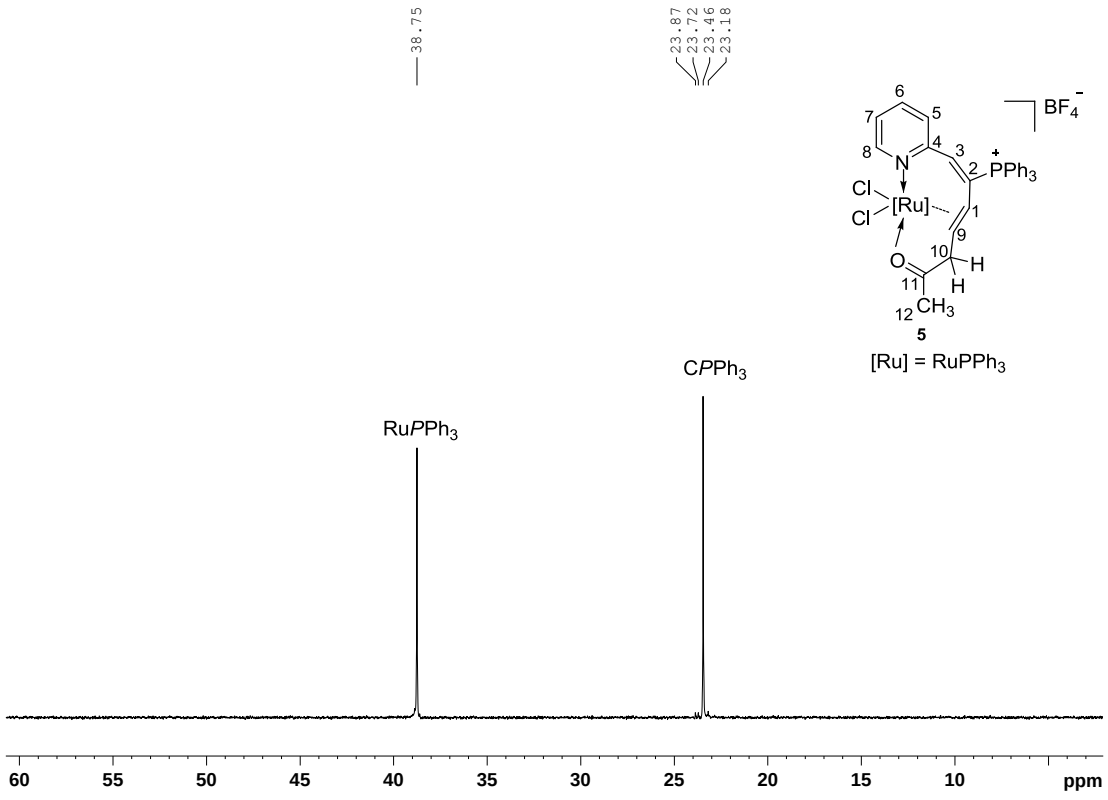

Figure S2-13 The ^{31}P NMR spectrum of complex **5** in CD_2Cl_2:$CDCl_3$ = 3:5 at 161.96 MHz.

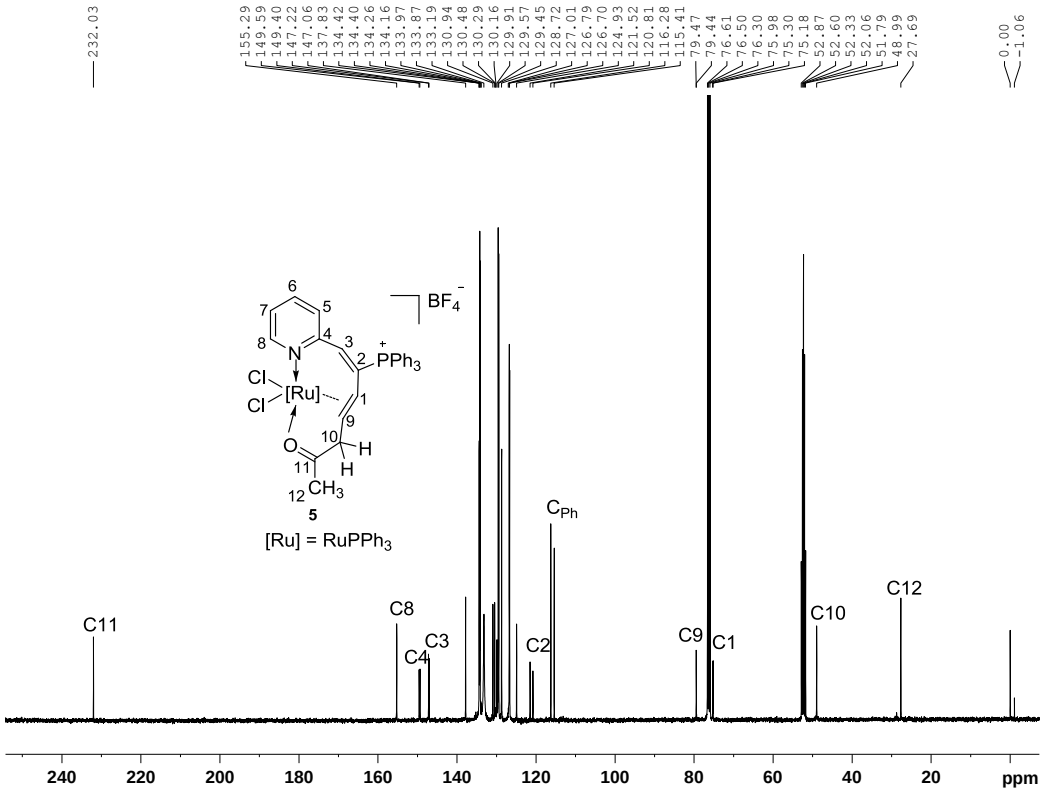

Figure S2-14 The ^{13}C NMR spectrum of complex **5** in CD_2Cl_2:$CDCl_3$ = 3:5 at 100.63 MHz.

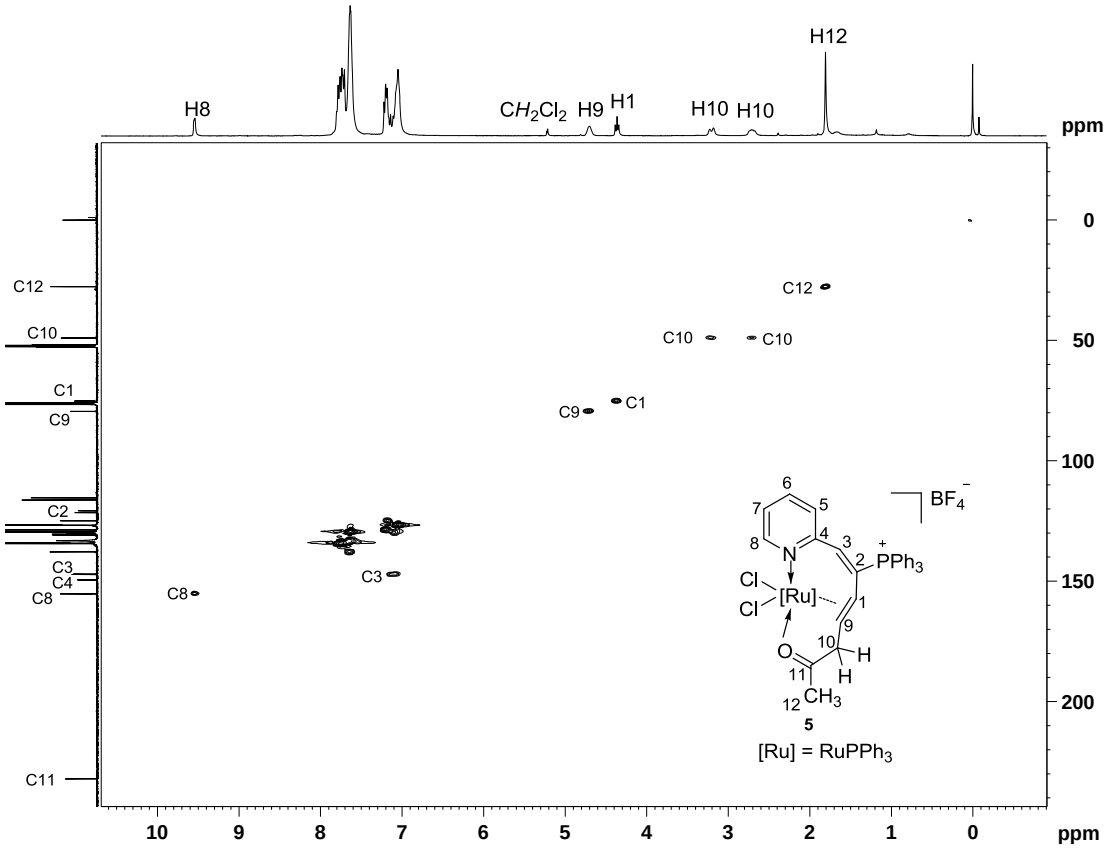

Figure S2-15 The ^{1}H–^{13}C HSQC of complex **5** in CD_2Cl_2:$CDCl_3$ = 3:5 at 100.63 MHz.

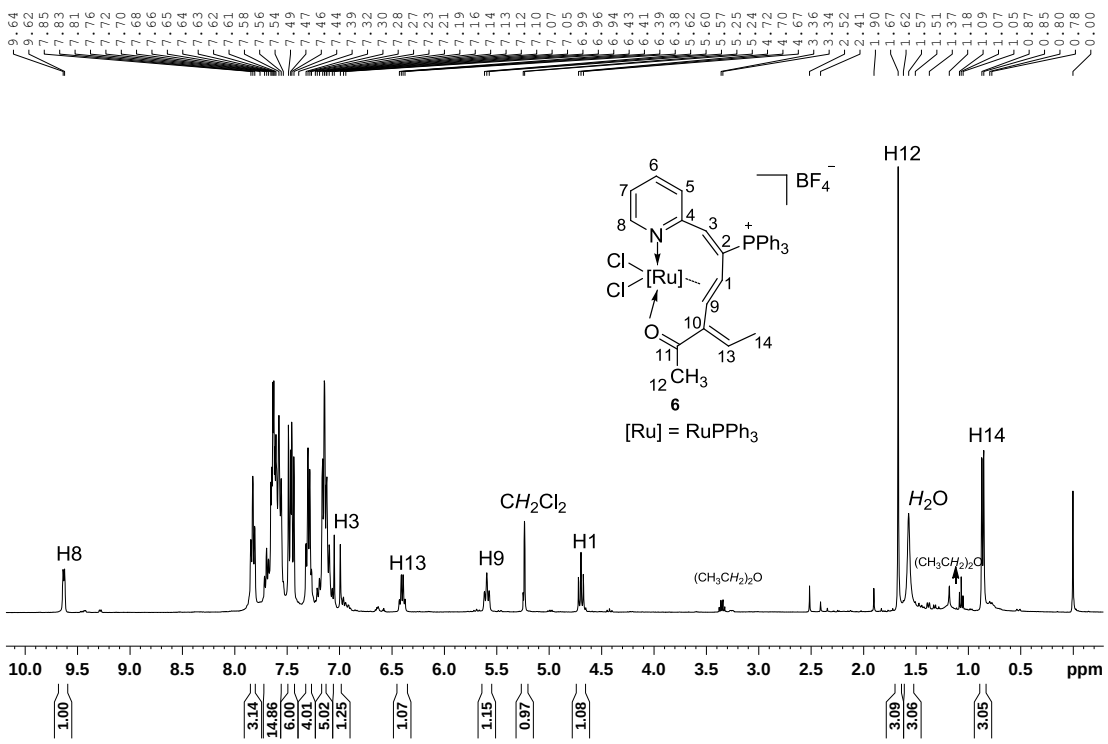

Figure S2-16 The ^{1}H NMR spectrum of complex **6** in CD_2Cl_2 at 400.13 MHz.

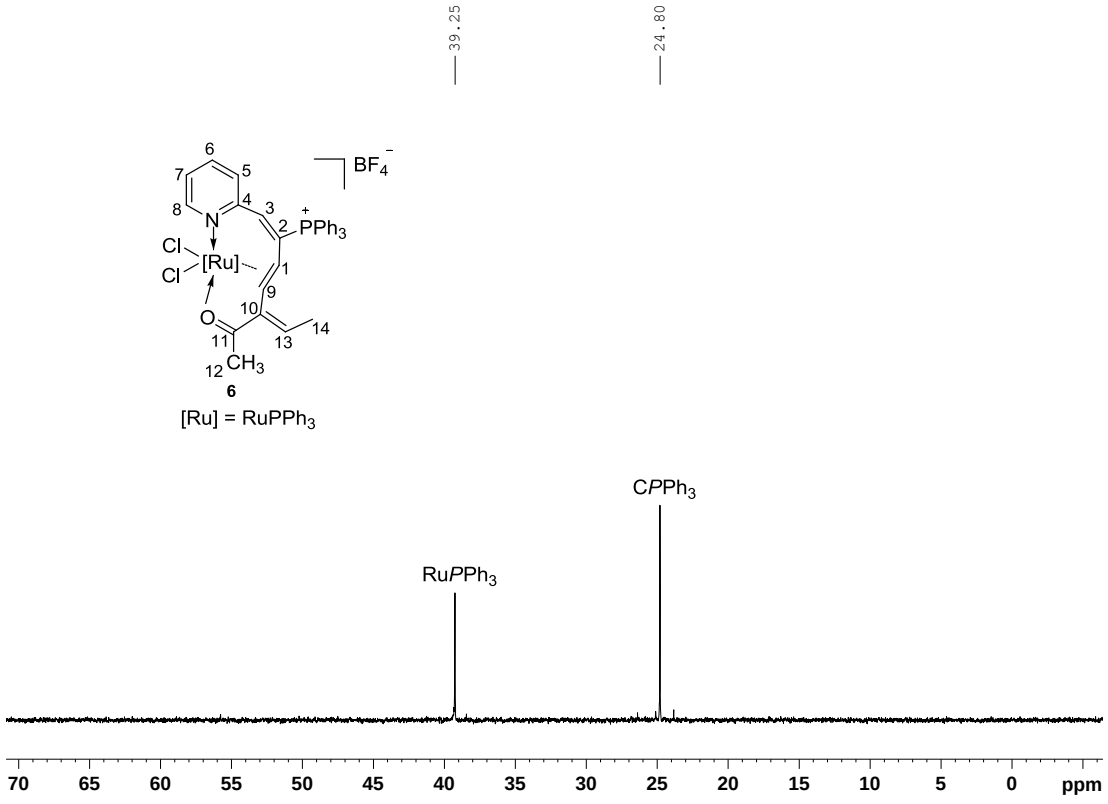

Figure S2-17 The ^{31}P NMR spectrum of complex **6** in CD_2Cl_2 at 161.96 MHz

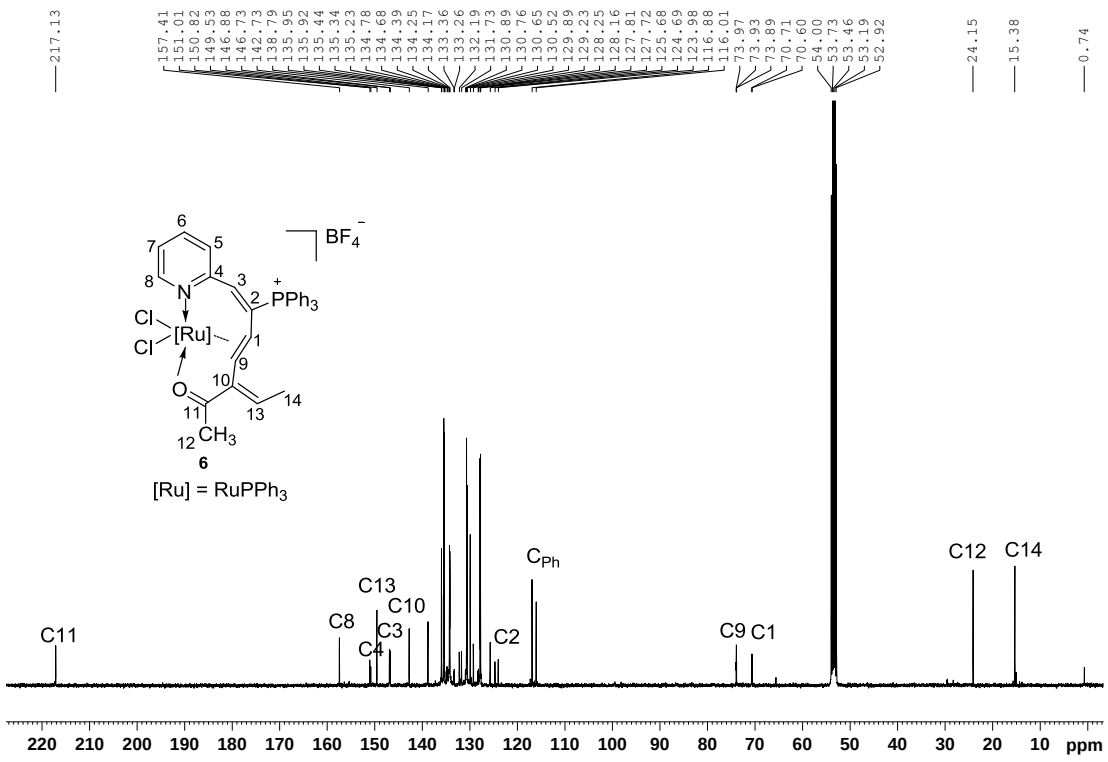

Figure S2-18 The ^{13}C NMR spectrum of complex **6** in CD_2Cl_2 at 100.63 MHz.

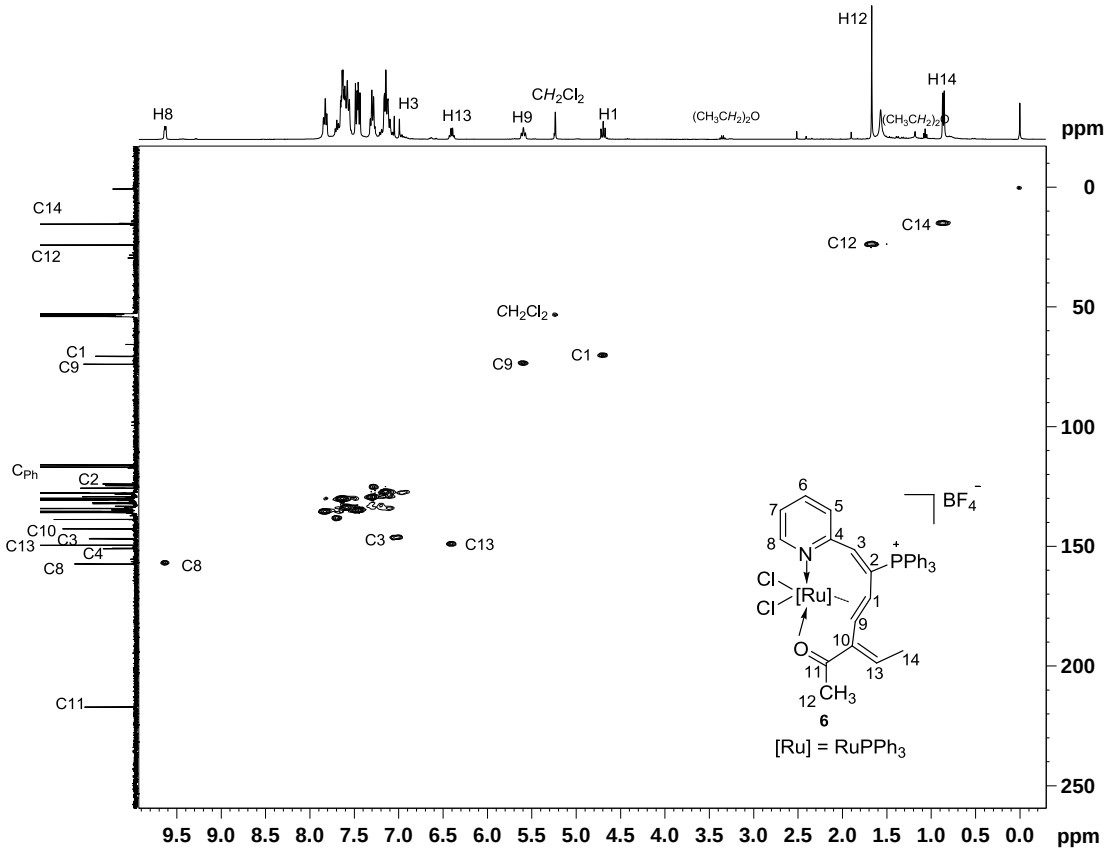

Figure S2-19 The ^{1}H-^{13}C HSQC spectrum for complex **6** in CD_2Cl_2 at 100.63 MHz.